BERKELEY ARCHAEOLOGICAL XRF LAB

Department of Anthropology
232 Kroeber Hall
University of California
Berkeley, CA 94720-3710

SOURCE PROVENANCE OF VOLCANIC ROCK CRUCIFORMS FROM THE ARIZONA STATE MUSEUM

by

M. Steven Shackley
Professor and Director
Geoarchaeological XRF Laboratory
University of California, Berkeley

Report Prepared for

Alan Ferg
Arizona State Museum
University of Arizona, Tucson

8 June 2011

INTRODUCTION

The analysis here of five volcanic rock cruciforms indicates that the majority were produced from intermediate volcanic rocks and one obsidian specimen. None of the samples could be assigned to source, although the obsidian specimen exhibits a peralkaline chemistry that is only present in northwestern Mexico, particularly Chihuahua and Sonora where many sources remain unlocated (Shackley 2005).

ANALYSIS AND INSTRUMENTATION

All archaeological samples are analyzed whole. The results presented here are quantitative in that they are derived from "filtered" intensity values ratioed to the appropriate x-ray continuum regions through a least squares fitting formula rather than plotting the proportions of the net intensities in a ternary system (McCarthy and Schamber 1981; Schamber 1977). Or more essentially, these data through the analysis of international rock standards, allow for inter-instrument comparison with a predictable degree of certainty (Hampel 1984).

Trace Element Analysis

The trace element analyses were performed in the NSF Geoarchaeological XRF Laboratory, Department of Anthropology, University of California, Berkeley, using a Thermo Scientific *Quant'X* energy dispersive x-ray fluorescence spectrometer. The spectrometer is equipped with a ultra-high flux peltier air cooled Rh x-ray target with a 125 micron beryllium (Be) window, an x-ray generator that operates from 4-50 kV/0.02-1.0 mA at 0.02 increments, using an IBM PC based microprocessor and WinTrace™ 4.1 reduction software. The spectrometer is equipped with a 2001 min^{-1} Edwards vacuum pump for the analysis of elements below titanium (Ti). Data is acquired through a pulse processor and analog to digital converter. This is a significant improvement in analytical speed and efficiency beyond the former Spectrace 5000 and *QuanX* analog systems (see Davis et al. 2011; Shackley 2005).

For Ti-Nb, Pb, Th elements the mid-Zb condition is used operating the x-ray tube at 30 kV, using a 0.05 mm (medium) Pd primary beam filter in an air path at 200 seconds livetime to

generate x-ray intensity $K\alpha_1$-line data for elements titanium (Ti), manganese (Mn), iron (as Fe^T), cobalt (Co), nickel (Ni), copper, (Cu), zinc, (Zn), gallium (Ga), rubidium (Rb), strontium (Sr), yttrium (Y), zirconium (Zr), niobium (Nb), lead (Pb), and thorium (Th). Not all these elements are reported since their values in many volcanic rocks is very low. Trace element intensities were converted to concentration estimates by employing a least-squares calibration line ratioed to the Compton scatter established for each element from the analysis of international rock standards certified by the National Institute of Standards and Technology (NIST), the US. Geological Survey (USGS), Canadian Centre for Mineral and Energy Technology, and the Centre de Recherches Pétrographiques et Géochimiques in France (Govindaraju 1994). Line fitting is linear (XML) for all elements but Fe where a derivative fitting is used to improve the fit for iron and thus for all the other elements. When barium (Ba) is acquired, the Rh tube is operated at 50 kV and 0.5 mA in an air path at 200 seconds livetime to generate x-ray intensity $K\alpha_1$-line data, through a 0.630 mm Cu (thick) filter ratioed to the bremsstrahlung region (see Davis et al. 2011). Further details concerning the petrological choice of these elements in North American obsidians is available in Shackley (1988, 1990, 1995, 2005; also Mahood and Stimac 1991; and Hughes and Smith 1993). A suite of 17 specific standards used for the best fit regression calibration for elements Ti- Nb, Pb, and Th, include G-2 (basalt), AGV-2 (andesite), GSP-2 (granodiorite), SY-2 (syenite), BHVO-2 (hawaiite), STM-1 (syenite), QLO-1 (quartz latite), RGM-1 (obsidian), W-2 (diabase), BIR-1 (basalt), SDC-1 (mica schist), BCR-2 (basalt), TLM-1 (tonalite), SCO-1 (shale), all US Geological Survey standards, NBS-278 (obsidian) from the National Institute of Standards and Technology, BR-1 (basalt) from the Centre de Recherches Pétrographiques et Géochimiques in France, and JR-1 and JR-2 (obsidian) from the Geological Survey of Japan (Govindaraju 1994).

Major Oxide Analysis

In order to determine the volcanic rock type, all five samples were subjected to a major oxide analysis, and then plotted on an alkali-silica plot (Figure 1). Analysis of the major oxides

of Si, Al, Ca, Fe, K, Mg, Mn, Na, and Ti is performed under the multiple conditions elucidated below. This fundamental parameter analysis (theoretical with standards), while not as accurate as destructive analyses (pressed powder and fusion disks) is usually within a few percent of actual, based on the analysis of USGS RGM-1 obsidian standard (see also Shackley 2011a). The fundamental parameters (theoretical) method is run under conditions commensurate with the elements of interest and calibrated with four USGS standards (RGM-1, rhyolite; AGV-2, andesite; BHVO-1, hawaiite; BIR-1, basalt), and one Japanese Geological Survey rhyolite standard (JR-1). Multiple conditions are designed to ameliorate peak overlap identified with digital filter background removal, least squares empirical peak deconvolution, gross peak intensities and net peak intensities above background. Current is set automatically based on the mass absorption coefficient.

Low Za (Na, Mg, Al, Si, P)

Voltage	6 kV	Current	Auto[2]
Livetime	100 seconds	Counts Limit	0
Filter	No Filter	Atmosphere	Vacuum
Maximum Energy	10 keV	Count Rate	Low

Low Zb (S, Cl, K, Ca)

Voltage	8 kV	Current	Auto
Livetime	100 seconds	Counts Limit	0
Filter	Cellulose (0.06 mm)	Atmosphere	Vacuum
Maximum Energy	10 keV	Count Rate	Low

Mid Zb (K, Ca, Ti, V, Cr, Mn, Fe)

Voltage	32 kV	Current	Auto
Livetime	100 seconds	Counts Limit	0
Filter	Pd (0.06 mm)	Atmosphere	Vacuum
Maximum Energy	40 keV	Count Rate	Medium

The data from the WinTrace software were translated directly into Excel for Windows and into SPSS for statistical manipulation. In order to evaluate these quantitative determinations, machine data were compared to measurements of known standards during each run (Tables 1 and 2). RGM-1 is analyzed during each sample run for obsidian artifacts to check machine calibration (Tables 1 and 2). Obsidian source investigation made by reference to source data at Berkeley and Shackley (1995, 2005, 2009a, 2009b), and Martynec et al. (2011).

DISCUSSION

OBSIDIAN ARTIFACT

The green/gray obsidian cruciform (Sample A-24180) exhibits a very similar elemental composition and megascopic character to Los Sitios del Agua in northern Sonora on the eastern edge of the Sierra Pinacate Volcanic Field south of Los Vidrios, formerly called “AZ Unknown A” (Martynec et al. 2011; Shackley 1995, 2005). However, none of the elemental concentrations match the nearly 50 samples standards reported for this source (Martynec et al. 2011; Shackley 2005; Figure 2 here). There are no known peralkaline (Al < Na+K) obsidian sources north of the border, but many south of the border, including Los Sitios del Agua, and most in Chihuahua (Shackley 2005; see Table 1 here). It is rational to infer that the source for this cruciform is somewhere in Sonora or Chihuahua.

INTERMEDIATE VOLCANIC ARTIFACTS

Based on the oxide analysis, the other four cruciforms were produced from intermediate volcanics from an andesite to trachy-andesite to trachy-dacite. These rocks occur throughout the

North American Southwest, indeed throughout western North America. Little more can be said about the provenance of these sources in the absence of source data (see Shackley 2011b).

REFERENCES CITED

Davis, M.K., T.L. Jackson, M.S. Shackley, T. Teague, and J. Hampel
2011 Factors Affecting the Energy-Dispersive X-Ray Fluorescence (EDXRF) Analysis of Archaeological Obsidian. In *X-Ray Fluorescence Spectrometry (XRF) in Geoarchaeology*, edited by M.S. Shackley, pp. 45-64. Springer, New York.

Govindaraju, K.
1994 1994 Compilation of Working Values and Sample Description for 383 Geostandards. *Geostandards Newsletter* 18 (special issue).

Hampel, Joachim H.
1984 Technical Considerations in X-ray Fluorescence Analysis of Obsidian. In *Obsidian Studies in the Great Basin*, edited by R.E. Hughes, pp. 21-25. Contributions of the University of California Archaeological Research Facility 45. Berkeley.

Hildreth, W.
1981 Gradients in Silicic Magma Chambers: Implications for Lithospheric Magmatism. *Journal of Geophysical Research* 86:10153-10192.

Hughes, Richard E., and Robert L. Smith
1993 Archaeology, Geology, and Geochemistry in Obsidian Provenance Studies. *In Scale on Archaeological and Geoscientific Perspectives*, edited by J.K. Stein and A.R. Linse, pp. 79-91. Geological Society of America Special Paper 283.

Le Bas, M.J., R.W. Le Maitre, A.L. Streckeisen, and B. Zanettin
1991 A Chemical Classification of Volcanic Rocks Based on the Total Alkali-Silica Diagram. *Journal of Petrology* 27:745-750

Mahood, Gail A., and James A. Stimac
1991 Trace-Element Partitioning in Pantellerites and Trachytes. *Geochemica et Cosmochimica Acta* 54:2257-2276.

Martynec, R., Davis, R., and M.S. Shackley
2011 The Los Sitios del Agua Obsidian Source (Formerly AZ Unknown A) and Recent Archaeological Investigations Along the Rio Sonoyta, Northern Sonora. *Kiva* 76(4), in press.

McCarthy, J.J., and F.H. Schamber
1981 Least-Squares Fit with Digital Filter: A Status Report. In *Energy Dispersive X-ray Spectrometry*, edited by K.F.J. Heinrich, D.E. Newbury, R.L. Myklebust, and C.E. Fiori, pp. 273-296. National Bureau of Standards Special Publication 604, Washington, D.C.

Schamber, F.H.
1977 A Modification of the Linear Least-Squares Fitting Method which Provides Continuum Suppression. In *X-ray Fluorescence Analysis of Environmental Samples*, edited by T.G. Dzubay, pp. 241-257. Ann Arbor Science Publishers.

Shackley, M. Steven

1988 Sources of Archaeological Obsidian in the Southwest: An Archaeological, Petrological, and Geochemical Study. *American Antiquity* 53(4):752-772.

1990 *Early Hunter-Gatherer Procurement Ranges in the Southwest: Evidence from Obsidian Geochemistry and Lithic Technology*. Ph.D. dissertation, Arizona State University, Tempe.

1995 Sources of Archaeological Obsidian in the Greater American Southwest: An Update and Quantitative Analysis. *American Antiquity* 60(3):531-551.

2005 *Obsidian: Geology and Archaeology in the North American Southwest*. University of Arizona Press, Tucson.

2009a The Topaz Basin Archaeological Obsidian Source in the Transition Zone of Central Arizona. *Geoarchaeology* 24:336-347.

2009b Two Newly Discovered Sources of Archaeological Obsidian in the Southwest. *Kiva* 76:269-280.

2011a An Introduction to X-Ray Fluorescence (XRF) Analysis in Archaeology. In *X-Ray Fluorescence Spectrometry (XRF) in Geoarchaeology*, edited by M.S. Shackley, pp. 7-44. Springer, New York.

2011b Sources of Archaeological Dacite in Northern New Mexico. *Journal of Archaeological Science* 38:1001-1007.

Table 1. Major oxide analysis of archaeological samples. All measurements in weight percent.

Sample	SiO_2	Al_2O_3	CaO	Fe_2O_3	K_2O	MgO	MnO	Na_2O	TiO_2	Rock type
A-3102	61.503	13.254	4.635	6.973	4.558	2.857	0.13	4.359	0.72	trachy-dacite
A-14987-X-2	68.025	13.204	2.517	5.577	4.707	0.266	0.106	4.363	0.574	trachy-dacite
A-14987-X-3	58.917	20.333	0.703	5.675	8.034	2.379	0.038	2.222	0.984	trachy-andesite
A-24180	73.057	9.978	0.568	3.49	7.927	0.519	0.117	3.65	0.153	rhyolite obsidian
A-36785-X-1	62.393	15.433	6.423	5.366	1.539	2.722	0.158	4.016	0.757	andesite
RGM1-S4	74.506	12.159	1.489	2.317	5.167	0	0.056	3.802	0.269	standard

Table 2. Minor and trace element analysis of archaeological samples. All measurements in parts per million (ppm).

Sample	Ti	Mn	Fe	Zn	Rb	Sr	Y	Zr	Nb	Ba	Pb	Th
A-3102	3217	602	32288	286	109	286	34	527	14	1902	32	3
A-14987-X-2	2686	547	27357	110	128	197	42	577	19	2301	14	9
A-14987-X-3	5166	234	32226	156	233	175	51	244	26	3396	44	24
A-24180	1181	558	18806	185	129	10	63	566	41	0	63	16
A-36785-X-1	3406	615	24641	122	35	2339	13	217	9	2360	51	3
RGM1-S4	1652	299	13263	35	149	109	25	218	11	809	20	18

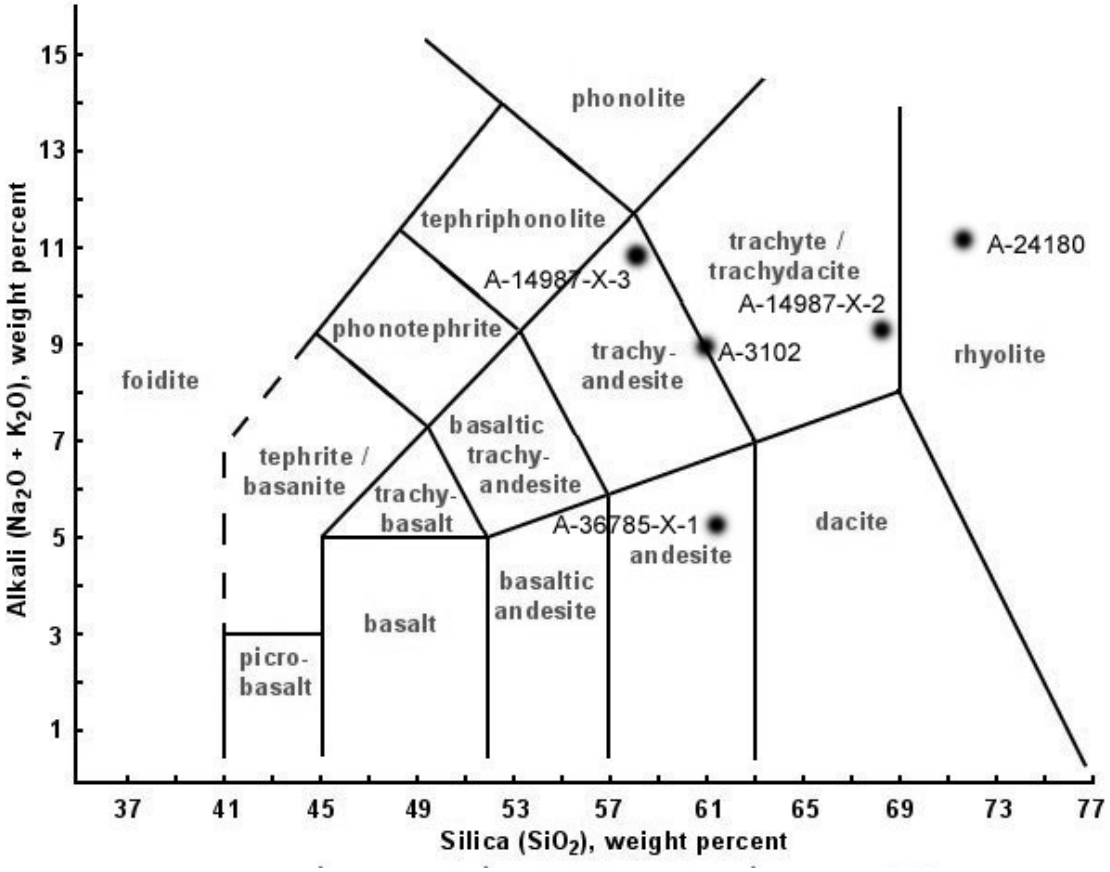

Figure 1. TAS plot of the archaeological specimens (based on Le Bas et al. 1986).

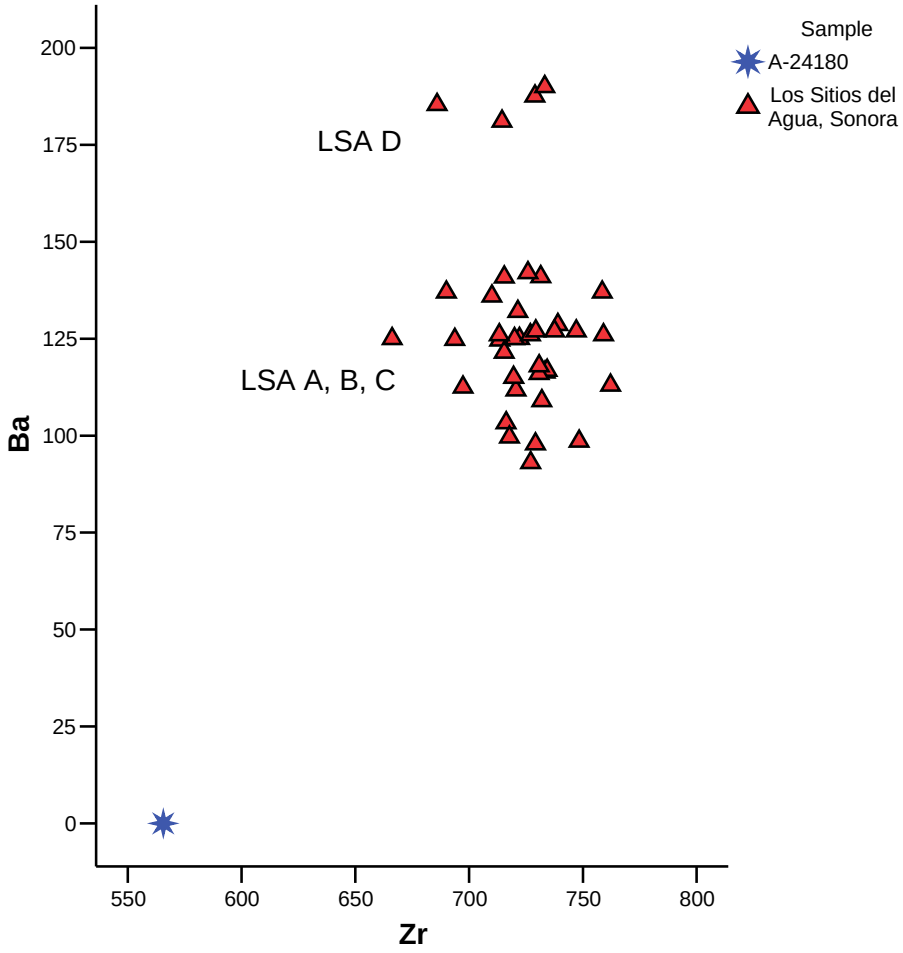

Figure 2. Zr versus Ba bivariate plot of the obsidian sample 24180 and the two Los Sitios del Agua source groups.